

# Evaluation of the spin diffusion length of AuW alloy by spin absorption experiments in the limit of large spin-orbit interactions

P. Laczkowski,<sup>1</sup> H. Jaffrès,<sup>1</sup> W. Savero-Torres,<sup>2,3</sup> J.-C. Rojas-Sánchez,<sup>1</sup> Y. Fu,<sup>2,3</sup> N. Reyren,<sup>1</sup> C. Deranlot,<sup>1</sup> L. Notin,<sup>2,3</sup> C. Beigné,<sup>2,3</sup> J.-P. Attané,<sup>2,3</sup> L. Vila,<sup>2,3</sup> J.-M. George,<sup>1</sup> and A. Marty<sup>2,3</sup>

<sup>1</sup>*Unité Mixte de Physique CNRS/Thales and Université Paris-Sud 11, 91767 Palaiseau, France*

<sup>2</sup>*Université Grenoble Alpes, INAC-SP2M, F-38000 Grenoble, France*

<sup>3</sup>*CEA, INAC-SP2M, F-38000 Grenoble, France*

(Dated: May 15, 2022)

The knowledge of the spin diffusion length  $\lambda_A$  is a prerequisite for the estimation of the spin Hall angle. We investigate spin current absorption of materials with small  $\lambda_A$  using AuW stripes inserted in lateral spin-valves. Width variations of the AuW stripe lead to drastic changes of the spin absorption, which cannot be explained by conventional analysis. We show that the spin-current polarization and the spin accumulation attenuation in the vicinity of the spin absorber must to be precisely taken into account for accurate estimation of  $\lambda_A$ . We propose an analytical model supported by numerical calculations that allows to extract proper  $\lambda_A$  values of spin Hall effect materials.

Recent developments in spin-orbitronics have brought an increased attention to the possibility of the efficient control of magnetization, as well as the creation of a lateral charge current through bulk or surface effects, resulting from strong spin-orbit interactions and the spin-orbit assisted scattering [1–5]. New materials and/or interfaces exhibiting large spin Hall angles (SHA) [6–10], as well as carefully engineered Rashba type interfaces [11, 12] and particular Fermi surface topologies [13] have opened an access to an efficient spin/charge current conversion. Moreover, the conversion ratio can be precisely tuned either by controlling the impurity level [14–17] or the gate voltage [18, 19], or even through the magnetization control of a substrate by transverse spin absorption at spin-active magnetic insulator interfaces [20].

Several methods such as Ferromagnetic-Resonance/Spin-Pumping [21–23], Spin Torque-Ferromagnetic Resonance [10], second harmonic Hall measurements [24] or Lateral Spin Valves (LSV) [25] allow extraction of the SHA. However the reported values are spread over one order of magnitude [26]. Moreover, in order to estimate the SHA of a given material, its spin diffusion length (SDL) must be perfectly known *e.g. via* comparative non-local spin signal measurements (spin sink experiments) or thickness dependence in spin Hall effect (SHE)/Spin-Pumping experiments [26–29].

As for for the latter, for the smallest thicknesses it is challenging to grow continuous and homogeneous films necessary for short SDL characterization thus precluding the use of this technique. In contrast, the LSVs with non-local spin-sink experiments provide an efficient alternative and they are proven to be efficient for short SDL materials [25, 31]. To extract the SDL, simulation by Finite Element Method (FEM) is a pertinent approach when dealing with short SDLs [7]. However, the exact knowledge of spin-current pathways in the limit of short SDLs requires a heavy mesh density and enormous computation power especially when combined with complex

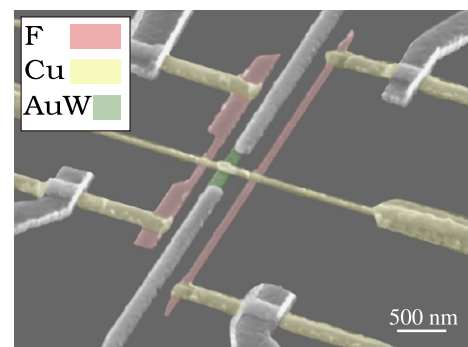


Figure 1. *Scanning electron microscope image of a typical lateral spin valve nano-device with inserted spin absorber AuW nano-wire fabricated using multi-angle evaporation technique [30].*

structures such as the ones presented here.

In this paper we present experimental data and the analysis of spin absorption in LSVs with a metallic AuW absorber [32] (13.8% at. W concentration in Au host). The analysis is based on an extended 1D spin absorption model which takes into account the spin-current polarization (SCP) and the spin accumulation (SA) profiles along the width of the inserted spin-absorber  $w_A$ . We demonstrate that for the short SDLs found in the AuW, when  $w_A$  becomes comparable to the effective SDL of the non-magnetic channel (N), lateral spread of the SCP and the sa in the AuW stripe need to be considered in the analysis. This spread becomes relevant when the spin-resistance of the spin-absorber  $R_A$  becomes smaller than the spin-resistance of the non-magnetic channel  $R_N$ . We show that when not considered this effect can lead to significant errors in the evaluation of  $\lambda_A$ , capable of reaching 90% in the present case. Therefore, we propose an extended model taking into account geometrical renormalization and we use it to extract a robust value of  $\lambda_A$  for  $AuW_{13.8\%}$  alloy independent of its width  $w_A$ .

In our experiments we use metallic LSVs with transparent interfaces. Figure 1 represents a scanning electron microscope image of a typical LSV device fabricated using the multi-angle nano-fabrication method [30], where the red color represents the ferro-magnetic (Py), yellow the non-magnetic (N) and green the spin absorber (A) material. First, the middle  $AuW_{13.8\%}$  wire is deposited on the  $SiO_2$  substrate using Physical Vapor Deposition and the lift-off technique, followed by the nano-fabrication of a  $Py/Cu$  LSV. In-between these two steps the middle wire surface is cleaned using Ar ion-milling. The Py, Cu and  $AuW_{13.8\%}$  nano-wires are 20 nm, 77 nm and 30 nm thick ( $t$ ) respectively. Their width is fixed to 50 nm with the exception of the  $AuW_{13.8\%}$  nano-wire whose width was varied ( $w_A = 45, 95, 195$  nm) in order to modulate the spin absorption. The distance separating the ferromagnetic electrodes is  $L = 600$  nm whereas the spin-sink is placed exactly in the middle. Resistivities of the materials used are given in the supplementary materials (SM).

In these experiments we follow the same protocol as for the SDL evaluation presented in our previous work [32, 33]. Non-local measurements have been performed for two types of nano-structures: the regular non-local device [Fig. 2(a)] and the non local device containing a  $AuW_{13.8\%}$  wire inserted in between the ferromagnetic electrodes [Fig. 2(b)]. As a result, clear spin signals were observed for both types of devices, the reference (blue) and the one with inserted SHE nano-wire (red). Their amplitudes were measured to be  $\Delta R_{ref} = 1.45$  m $\Omega$  and  $\Delta R_{abs} = 0.22$  m $\Omega$  (for  $w_A = 45$  nm) respectively [Fig. 2(c)]. This indicates a strong spin absorption of the spin accumulation and correlated strong reduction of the spin-current by the AuW wire, reducing thus the amplitude of the spin signal. Also, the amplitude of the spin signal was studied as a function of the AuW nano-wire width, yielding  $\Delta R_{abs} = 220$   $\mu\Omega$ , 19.5  $\mu\Omega$ , 5.6  $\mu\Omega$  for  $w_A = 45, 140, 195$  nm respectively, and as a consequence a clear exponential decay of  $\Delta R_{abs}$  as a function of increasing  $w_A$  is observed [Fig. 2(d)].

By comparing  $\Delta R_{ref}$  with  $\Delta R_{abs}$  and using the resistivity of the inserted AuW wire  $\rho_A = 1040$   $\Omega.nm$  [33] one can evaluate properly its spin diffusion length. For this purpose a commonly used 1D model approach presented in [6, 7] was used [34]. We define the spin resistances for the ferro-magnets, the non-magnet and the spin absorber respectively:  $R_F = \frac{\rho_F \lambda_F}{(1-\beta^2)w_F w_N}$ ,  $R_N = \frac{\rho_N \lambda_N}{w_N t_N}$ ,  $R_A = \frac{\rho_A \lambda_A}{w_A w_N}$ . The values of  $\lambda_A$  extracted from conventional analysis as a function of  $w_A$  are summarized in the table I:

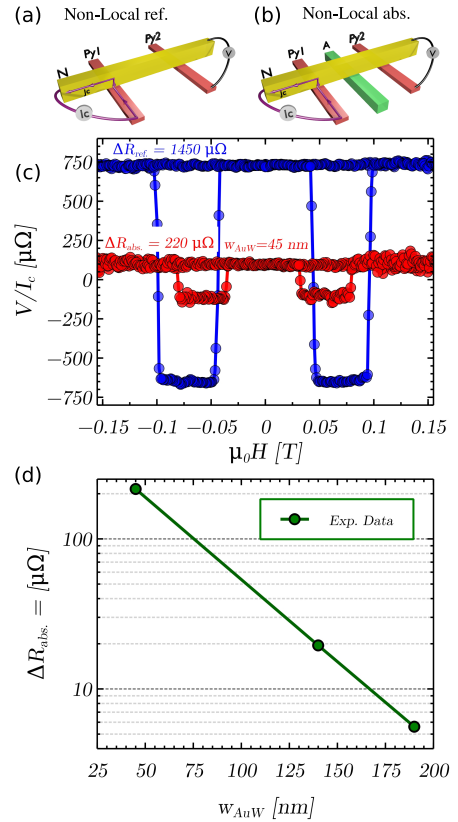


Figure 2. Schematic representations of spin-sink experiment for (a) reference (without AuW wire) and (b) absorption (with inserted AuW wire) nano-devices measured in the non-local probe configuration. (c) Non-local measurements of reference (blue) and absorption (red) devices recorded at  $T = 9$  K for ferromagnetic electrode separation of  $L = 600$  nm (from the center of Py1 to the center of Py2) and  $w_A = 45$  nm. (d) Amplitude of the spin signal of the absorption device in the non-local probe configuration as a function of the AuW nano-wire width.

$w_A$ [nm]	45	140	195
$\lambda_A$ [nm]	1.32	0.30	0.10

Table I. The spin diffusion length of the  $AuW_{13.8\%}$  nano-wire  $\lambda_A$  for three different  $w_A$  estimated by using the 1D point-contact spin absorption model.

Contrary to what might be expected, different values of  $\lambda_A$  were found depending on the  $w_A$  for the same W concentration. In particular for the larger AuW wires an extremely short  $\lambda_A$  was evaluated (of about 0.1 nm), which has no physical meaning except indicating a larger effective efficiency of spin absorption. The variation of  $\lambda_A$  as a function of  $w_A$  can be understood when considering that the level of spin accumulation probed by the AuW wire is not the same depending on its width. Until now, in the state-of-the-art literature the lateral size

of the contacts were considered much smaller than the channel SDL ( $w_A \ll \lambda_N$ ) for which reason the spin-sink has been considered as a point-contact source of spin absorption [35]. The formula which describes spin-signals in multiterminal devices corresponding to a two points or three points geometry explored for the local or the non-local  $MR$  and the spin Hall effect experiments, have been derived using such an assumption. However, as the width of the spin-sink becomes of the same order of magnitude as the channels  $SDL$  ( $w_A \sim \lambda_N$ ), as in the present case ( $\lambda_N \sim 380 \text{ nm}$  compared to  $w_{A-max} \sim 200 \text{ nm}$ ) or even larger, this ceases to be valid. This is because the SCP and the SA profiles cannot be assumed to be uniform as usual, due to their exponential dependence on the profile variation in the non-magnetic channel above the spin absorber. Indeed, a contact size larger than the channel SDL leads to an exponential increase of the spin absorption at the edge. Therefore, we propose a new criterium for that model and demonstrate that the situation is even more complex and a significant correction could also be required in the limit of the long  $\lambda_N$  [SM]. Further we will refer to the commonly used formula [25] as a point-contact model [36]. Schematic representation of this approach [37] is shown in Fig. 3(a).

In order to describe our experiments and obtain a robust value of  $\lambda_A$  we have developed extended 1D calculations taking into account the SCP and the SA in the AuW nano-wire. We have then considered two approaches in order to model the AuW nanowire as represented in Fig. 3(b), namely the Matrix and the Resistor models described in detail below. We will demonstrate these models to be equivalent. In both of them we did not consider any lateral spin current in the spin-sink because of its short  $\lambda_A$ .

This first approach consists of the discretization of an inserted AuW nano-wire in a series of ' $N$ ' neighboring contacts, each of them being a source of spin-absorption. The 1D extended model [Fig. 3(a)] is based on the transfer matrix model [35] adapted to the case of spin transport in both local and non-local probe configurations in LSVs, developed in our previous work [35, 38] and explained in details in the supplementary materials [SM]. The numerical discretization of the AuW spin-sink over the whole experimental series (width from 45 to 195 nm) into a collection of at least 9 smaller contacts of total equivalent size is sufficient. Larger discretization does not modify the spin signal, converging at a given value. The discrete elements are of a lateral size  $w_{min} \sim 20 \text{ nm}$  for the largest wire which will correspond to  $w_{min} = \lambda_{eff}/2$  [SM].

Moreover as a second approach, we have developed an analytical formulation based on the spin resistor model [37] which we have adapted to the case of a strong absorber. In such a case the part of the non-magnetic channel above the absorber was replaced by an effective spin resistor composed of a AuW/Cu material which was in

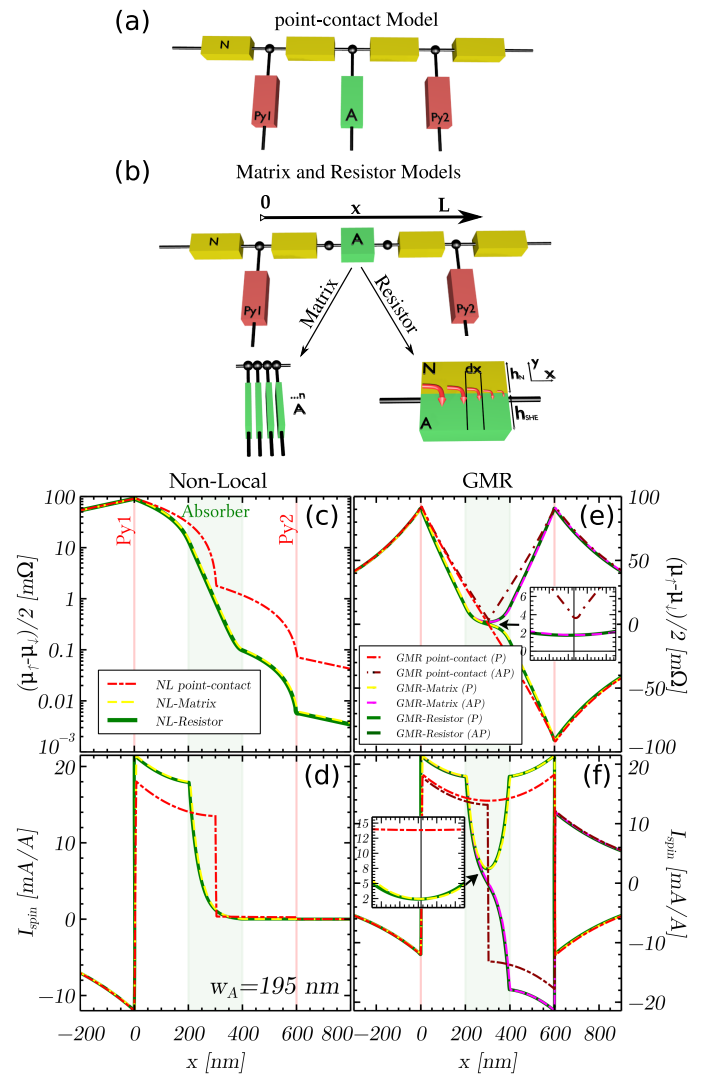


Figure 3. Schematic representation of (a) point-contact and (b) Matrix and Resistor models with two SHE resistor approaches represented on the bottom of the sketch. Profiles of spin accumulation (top) and current spin polarization (bottom) for point-contact (dash-dot), Matrix (dash) and Resistor (solid line) for (c-d) Non-Local and (e-f) GMR measurement configurations. Notations 'AP' and 'P' stand for the anti-parallel and parallel magnetic configuration of the Py injector/detector. The position of the injector (Py1) and the detector (Py2) as well as the spin absorber (Absorber) are identified by vertical lines.

parallel contact [Fig. 3(a)] and can be described by an effective spin diffusion length:  $\frac{1}{\lambda_{eff}^2} = \frac{1}{\lambda_N^2} + \frac{\rho_N}{\rho_A} \frac{th(\frac{t_A}{\lambda_A})}{\lambda_A t_N}$  [SM]. Thus, we can access a simple formula for the normalized spin signal  $\eta = \Delta R_{abs}/\Delta R_{ref}$  which was used to investigate limits of 1D models [SM].

We have compared the SA and the SCP profiles for the cases of a Non-Local [Fig. 3(b)] and GMR probe configuration [38] corresponding to our experimental geometry with  $w_A = 195 \text{ nm}$  [39]. Figure [Fig. 3(c-f)] displays

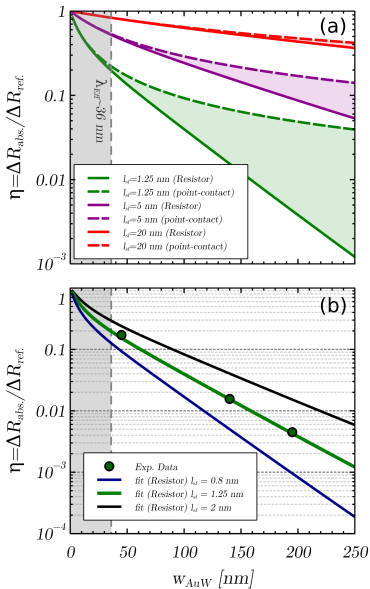


Figure 4. (a) Normalized spin signal amplitude  $\eta$  as a function of the width of the AuW nano-wire  $w_A$  represented for a case of three different spin diffusion lengths  $\lambda_A$ . Dashed line stands for point-contact while solid line stands for Resistor model. (b) AuW spin diffusion length fits using Resistor model (solid lines) to the experimental data (green points) plotted for three different cases. Grey region with dashed line indicates the limit where  $w_A < \lambda_{\text{eff}}$  [SM].

such profiles along the Cu channel. Both calculations (using the Resistor and the Matrix models) lead to the same profiles which highlight the validity of the analytical expression. We also checked that this match is valid for every considered geometry. In particular, in the non-local geometry, these calculations emphasize a decrease of 70% of the level of spin accumulation at the center of the spin-sink [Fig. 3(c)] together with a significant increase of the spin-current by 93% [Fig. 3(d)] at the same point due to the shorter effective SDL. However, in a standard GMR measurement configuration the SA decreases by about 82% in the AP state [inset Fig. 3(e)] whereas the SCP in the PA state drops by 80% [inset of Fig. 3(f)]. This should be correlated to a total decrease of the spin-signal by more than 90% [35] compared to conventional (point-contact) analysis. The conclusion is that obviously the point-contact approach appears as a very simple approximation for both SCP and SA profiles.

In order to get more insight on the limit of validity of the point-contact 1D model, we have compared the normalized spin signal  $\eta$  as a function of  $w_A$  from the two analytical models (point-contact and Resistor) represented schematically in Fig. 3(a-b). Figure 4(a) displays characteristic plots for three different cases of SDLs (denoted by different colors) for these models. Important differences between the point-contact model and the Resistor model are still present especially for the case of

short  $\lambda_A$  and in the limit where  $w_A \geq \lambda_N$ . Large corrections related to the SCP and SA profiles in the AuW wire need to be considered in order to avoid errors. For larger nano-wires  $w_A = 200$  nm the difference between the estimated  $\eta$  can be larger than 90% which will lead to an estimation of the  $\lambda_A \sim 0.1$  nm or less instead of more realistic value of  $\lambda_A \sim 1.25$  nm. Significant differences can be noticed for all  $\lambda_N < 2$   $\mu\text{m}$  while keeping  $R_N$  constant [SM]. These differences are however not so pronounced if we consider a longer  $\lambda_A \sim 14$  nm (when using  $\lambda_N \sim 1.5$   $\mu\text{m}$  and keeping  $R_N$  constant). We come to the conclusion that the geometrical renormalization of the spin signal (increased spin absorption) is necessary in the case of short  $\lambda_A$  (1.25 nm in the present case) even if  $\lambda_N$  is large (up to 1.5  $\mu\text{m}$ ) [SM].

The figure 4(b) displays the fit of the experimental data-points of  $\eta$  as a function of  $w_A$ , by using the 1D extended model (green line). The black and blue lines represent the case of different  $\lambda_A$  using the same model and are plotted to demonstrate the high precision which we get by using this type of estimation of  $\lambda_A$ . Moreover, we highlight the fact that a single and robust value of  $\lambda_A$  is obtained for three experimental data-points, as expected and that the extrapolation to  $w_A = 0$  nm allows to recover the spin-signal of the reference device  $\Delta R_{\text{ref}} = 1.45$  m $\Omega$ . Also, in contrast to the estimations from the point-contact approach, summarized in table I, this highlights the necessary correction as proposed in this paper.

In conclusion, we emphasize that the extraction of the SDL should be carefully addressed, particularly when the spin accumulation profile along the width of a spin absorber cannot be considered uniform any longer for large spin-sink sizes and especially for small  $\lambda_A$ . We have addressed this issue by developing adapted models taking into account this variation. The validity of this approach was experimentally proven by studying the absorption of the spin accumulation as a function of the  $\text{AuW}_{13.8\%}$  spin-absorber width in non-local spin valve experiments. We have demonstrated that the geometrical effects have to be considered with caution in the analysis of the spin-signals in non-local and local geometry for spin-sink experiments and we have refined the 1D model accordingly. Finally, we have presented a unique method which is well adapted to precisely determine short spin diffusion lengths by studying the width dependence of the spin current absorption in Non-Local Spin Valves with the inserted spin-absorber.

Samples were fabricated in the Plateforme *Technologie Avancee* in Grenoble, for which we acknowledge the support of the Renatec network. This work was supported by the ANR simi 10 SOspin project.

- 
- [1] S. S. P. Parkin, M. Hayashi, and L. Thomas, *Science* **320**, 190 (2008).
- [2] I. M. Miron, K. Garello, G. Gaudin, P.-J. Zermatten, M. V. Costache, S. Auffret, S. Bandiera, B. Rodmacq, A. Schuhl, and P. Gambardella, *Nature* **476**, 189 (2011).
- [3] M. Cubukcu, O. Boulle, M. Drouard, K. Garello, C. O. Avci, I. M. Miron, J. Langer, B. Ocker, P. Gambardella, and G. Gaudin, *Applied Physics Letters* **104**, 042406 (2014).
- [4] S. Parkin and S.-H. Yang, *Nature Nanotechnology* **10**, 195 (2015).
- [5] X. Qiu, K. Narayanapillai, Y. Wu, P. Deorani, D.-H. Yang, W.-S. Noh, J.-H. Park, K.-J. Lee, H.-W. Lee, and H. Yang, *Nature Nanotechnology* **10**, 333 (2015).
- [6] Y. Niimi, M. Morota, D.H. Wei, C. Deranlot, M. Basletic, A. Hamzic, A. Fert, and Y.C. Otani, *Physical Review Letters* **106**, 126601 (2011).
- [7] Y. Niimi, Y. Kawanishi, D.H. Wei, C. Deranlot, H.X. Yang, M. Chshiev, T. Valet, A. Fert, and Y.C. Otani, *Physical Review Letters* **109**, 156602 (2012).
- [8] K. Fujiwara, Y. Fukuma, J. Matsuno, H. Idzuchi, Y. Niimi, Y.C. Otani, and H. Takagi, *Nature Communications* **4** (2013), 10.1038/ncomms3893.
- [9] Y. Niimi, H. Suzuki, Y. Kawanishi, Y. Omori, T. Valet, A. Fert, and Y.C. Otani, *Physical Review B* **89**, 054401 (2014).
- [10] L. Liu, T. Moriyama, D.C. Ralph, and R.A. Buhrman, *Physical Review Letters* **106**, 036601 (2011).
- [11] J. R. Sánchez, L. Vila, G. Desfonds, S. Gambarelli, J. Attané, J. De Teresa, C. Magén, and A. Fert, *Nature Communications* **4** (2013), 10.1038/ncomms3944.
- [12] J. Borge, C. Gorini, G. Vignale, and R. Raimondi, *Physical Review B* **89**, 245443 (2014).
- [13] J. E. Moore, *Nature* **464**, 194 (2010).
- [14] A. Fert, A. Friederich, and A. Hamzic, *Journal of Magnetism and Magnetic Materials* **24**, 231 (1981).
- [15] A. Fert and P. M. Levy, *Physical Review Letters* **106**, 157208 (2011).
- [16] M. Gradhand, D. V. Fedorov, P. Zahn, and I. Mertig, *Physical Review B* **81**, 245109 (2010).
- [17] M. Gradhand, D. V. Fedorov, P. Zahn, and I. Mertig, *Solid State Phenomena* **168**, 27 (2011).
- [18] A.D. Caviglia, M. Gabay, S. Gariglio, N. Reyren, C. Cancellieri, and J.-M. Triscone, *Physical Review Letters* **104**, 126803 (2010).
- [19] X. He, T. Guan, X. Wang, B. Feng, P. Cheng, L. Chen, Y. Li, and K. Wu, *Applied Physics Letters* **101**, 123111 (2012).
- [20] F.K. Dejene, N. Vlietstra, D. Luc, X. Waintal, J. BenYoussef, and B.J. van Wees, *Physical Review B* **91**, 100404 (2015).
- [21] K. Ando and E. Saitoh, *Journal of Applied Physics* **108**, 113925 (2010).
- [22] Y. Tserkovnyak, A. Brataas, G. E. Bauer, and B. I. Halperin, *Reviews of Modern Physics* **77**, 1375 (2005).
- [23] O. Mosendz, V. Vlaminck, J.E. Pearson, F.Y. Fradin, G.E.W. Bauer, S.D. Bader, and A. Hoffmann, *Physical Review B* **82**, 214403 (2010).
- [24] K. Garello, I. M. Miron, C. O. Avci, F. Freimuth, Y. Mokrousov, S. Blügel, S. Auffret, O. Boulle, G. Gaudin, and P. Gambardella, *Nature nanotechnology* **8**, 587 (2013).
- [25] T. Kimura, J. Hamrle, and Y.C. Otani, *Physical Review B* **72**, 014461 (2005).
- [26] J.-C. Rojas-Sánchez, N. Reyren, P. Laczkowski, W. Savero, J.-P. Attané, C. Deranlot, M. Jamet, J.-M. George, L. Vila, and H. Jaffrès, *Physical Review Letters* **112**, 106602 (2014).
- [27] H. Nakayama, K. Ando, K. Harii, T. Yoshino, R. Takahashi, Y. Kajiwara, K. Uchida, Y. Fujikawa, and E. Saitoh, *Phys. Rev. B* **85**, 144408 (2012).
- [28] A. Azevedo, L.H. Vilela-Leao, R.L. Rodríguez-Suárez, A.F. LacerdaSantos, and S.M. Rezende, *Physical Review B* **83**, 144402 (2011).
- [29] Z. Feng, J. Hu, L. Sun, B. You, D. Wu, J. Du, W. Zhang, A. Hu, Y. Yang, D. Tang, *et al.*, *Physical Review B* **85**, 214423 (2012).
- [30] P. Laczkowski, L. Vila, S. Ferry, A. Marty, J.-M. George, H. Jaffrès, A. Fert, T. Kimura, T. Yang, Y.C. Otani, *et al.*, *Applied Physics Express* **4**, 063007 (2011).
- [31] L. Vila, T. Kimura, and Y.C. Otani, *Physical Review Letters* **99**, 226604 (2007).
- [32] P. Laczkowski, J.-C. Rojas-Sánchez, W. Savero-Torres, H. Jaffrès, N. Reyren, C. Deranlot, L. Notin, C. Beigné, A. Marty, J.-P. Attané, *et al.*, *Applied Physics Letters* **104**, 142403 (2014).
- [33] P. Laczkowski, *Courants de spin et l'effet Hall de spin dans des nanostructures latérales*, Ph.D. thesis, Grenoble (2012).
- [34] The 1D model used in these references is a more advanced version of the one developed in [25]. However a factor of two in the extracted spin diffusion lengths can be systematically found between these two models, in the way that  $\lambda_A^{Kimura et al.} = 2 \times \lambda_A^{Niimi et al.}$ .
- [35] H. Jaffrès, J.-M. George, and A. Fert, *Physical Review B* **82**, 140408 (2010).
- [36] Note that the standard formula proposed in [25] was adapted to the case of short spin diffusion length of both ferromagnets and spin-absorber for comparison with proposed models [SM].
- [37] W. Savero-Torres, A. Marty, L. Vila, P. Laczkowski, M. Jamet, and J.-P. Attané, [arXiv:1506.01347](https://arxiv.org/abs/1506.01347).
- [38] P. Laczkowski, L. Vila, V.-D. Nguyen, A. Marty, J.-P. Attané, H. Jaffrès, J.-M. George, and A. Fert, *Physical Review B* **85**, 220404 (2012).
- [39] Note that the Non-Local configuration corresponds to injection of the current at left ferromagnetic wire and absorption at infinity whereas in the GMR probe configuration current is injected at left ferromagnetic wire and absorbed at the right ferromagnetic wire.